Int. J. Chem. Sci.: 11(3), 2013, 1299-1313
ISSN 0972-768X
www.sadgurupublications.com

BIOCHEMICAL STUDY FOR BISMUTH OXIDE AND TELLURIUM NANOPARTICLES ON THYROID HORMONE LEVELS IN SERUM AND SALIVA OF PATIENTS WITH CHRONIC RENAL FAILURE

A. M. NOORI JASSIM[*], F. F. MOHAMMED AL-KAZAZZ and A. KHALAF ALI[a]

Department of Chemistry, College of Science, The University of Mustansiryah, BAGHDAD, IRAQ
[a]School of Applied Sciences, University of Technology, Al-Mustansiriya University, BAGHDAD, IRAQ

ABSTRACT

Noble metals nanoparticles (NPs) were synthesized directly by pulsed laser ablation (Nd : YAG, λ = 1064 nm) of bismuth and tellurium plates immersed in pure water. Concentrations of the NPs were determined by Atomic Absorption Spectroscopy (AAS) measurement. Atomic Force Microscope (AFM) and Transmission Electron Microscope (TEM) analysis were used to characterize the size and size distributions of the metals NPs. The objective of this work is studying the effects of presence of these NPs on the levels of tri-iodothyronine hormone (T_3) in serum and saliva of patients with chronic renal failure (CRF) their thyroid had disorder (hypothyroidism). Also the study characterized the binding between the anti-T3 antibody with its antigen i.e., T_3 in serum and saliva patients in the presence affixed size concentration of NPs to improve and modify a competitive ELISA method.

It is found that both bismuth oxide and tellurium NPs demonstrated different effect (activation or inhibition) on the binding between anti-T3 antibody and antigen (T3) in the serum and saliva of patients and these effects were depending on the increasing of the concentrations and size for both NPs. In conclusion, both bismuth oxide and tellurium NPs can be useful in biomedical applications such as the treatment and follow up by adjustment the levels of thyroid hormones of patients suffered from thyroid disorder.

Key words: Nanoparticles, Bismuth oxide, Tellurium, Thyroid hormones, Chronic renal failure.

INTRODUCTION

Nanotechnology involves the characterization, fabrication and/or manipulation of structures, devices or materials that have at least one dimension (or contain components with at least one dimension) that is approximately 1-100 nm in length. When particle size is

[*]Author for correspondence; E-mail: kadirchem@yahoo.com, fatin.1964@yahoo.com

reduced below this threshold, the resulting material exhibits physical and chemical properties that are significantly different from the properties of macro scale materials composed of the same substance[1]. It is applied to various fields such as physical, chemical, biological and engineering sciences where novel techniques are being developed to probe and manipulate single atoms and molecules. Among all NPs the metallic one have applications in diverse areas such as electronics, cosmetics, coating, packaging and biotechnology[2]. NPs can traverse through the vasculature and localize any target organ, this leads to novel therapeutic, imaging and biomedical application[3]. Bismuth (Bi) is a metallic element of the VA group, together with nitrogen, phosphorus, antimony, and arsenic. Its oxidation numbers are +3 and +5. It is found in the same proportions as silver in the earth's crust, and it occupies the 73rd place in abundance[4]. Theoretical studies predicted that nano structured bismuth is potentially useful for optical, electrooptic device applications, enhanced thermoelectric feature and catalysts[5]. NPs have an increased surface area and therefore have increased interaction with biological targets[4].

Tellurium (Te) is a semiconductor and is frequently doped with copper, tin, gold or silver. It is used in metallurgy as a secondary vulcanizing agent for rubber, in color glass and ceramics, in alloying agent, small amount of Te are add to copper and stainless steel to make them easier to machine and mill. Possible future uses are Te-methionine as heavy-atom label for X-ray studies in proteins and enzymes, Te-agents in cancer drug development, Te-agents as (selective) antibiotics and TeNPs in medicine[6,7].

Alternative-novel, easy, fast and one-step (based on Pulsed Laser Ablation in Liquids medium denoted by PLAL) method for the preparation of pure and stable noble metal versatile NPs in a high ablation rate and size-selected manner with a high concentration, long period of stability, less aggregation, nontoxic and contamination[8]. In recent decades, laser ablation of a solid target in a liquid environment has been widely used in preparation of nanomaterials and fabrication of nanostructures. Remarkably, there are many groups that pay attention to this issue in the world, and a large variety of nanomaterials such as metals, metallic alloys, semiconductors, polymers, etc, have been synthesized using laser ablation of solid in liquid. Therefore, laser ablation in liquids has been recognized to be an effective and general route to synthesize nanocrystals and fabricate nanostructures[9]. Noble metal Bi_2O_3NPs and TeNPs are synthesized by using pulsed laser ablation (Q-switched, 1064 nm- Nd : YAG) of Bi and Te metal plates immersed in distilled deionized water (DDW).

The kidney normally plays an important role in the metabolism, degradation and excretion of several thyroid hormones. Chronic Renal Failure (CRF) affects thyroid function in many ways, including low circulating thyroid hormone levels, altered peripheral hormone

metabolism, insufficient binding to carrier proteins, and possible reduction in tissue hormone content and altered iodide storage in the thyroid gland[10]. Thus, patients with renal failure may have various abnormalities of thyroid function[11]. Tri-iodothyronine (T3) is a tyrosine derivative hormone synthesized and stored in the thyroid gland. More than 99% of T3 in the blood is bound reversibly to plasma proteins. The concentration of T3 is much lower than that of thyroxin T4, but its metabolic potency is much greater[12]. Saliva is watery substance produced in the mouths of humans and most other animals. Produced in and secreted from the three pairs of major and hundreds of minor salivary gland[13]. Saliva can be collected with or without stimulation. Unstimulated whole saliva is the mixture of the secretions, which enter the mouth in the absence of exogenous gustatory, masticatory or mechanical stimulation[14]. Interest in saliva as a diagnostic fluid has grown in recent years and monitoring of makers in saliva instead of serum is found to be advantageous[15]. The Enzyme-Linked Immuno Sorbent Assay (ELISA) is the technique most commonly used by molecular biologists for biomarker detection and quantification. ELISA tests are based on the principle of a solid phase enzyme-linked immunosorbent assay using the spectroscopic detection of a colored reagent[16,17]. The aims of the work are to preparation of more stable-dispersed and size-controlled of pure Bi_2O_3NPs and TeNPs in easy, fast and simple method with highly ablation efficiency and studying the effects of presence these NPs on the levels of T3 in sera and saliva patients with CRF whose their thyroid had hyperthyroidism and improved and modified a competitive ELISA method.

EXPERIMENTAL

Preparation and characterization of Bi_2O_3NPs and TeNPs

Bi_2O_3 NPs and TeNPs were prepared by irradiating a metallic target plates with a thickness of 1mm placed on the bottom of quartz vessel containing DDW with a pulsed laser beam. The ablation was performed with the 1064 nm of Nd : YAG laser (HUAFEI) operating at 10 Hz repetition rate, with a pulse width of 10 ns at energy set in (500, 600, 700) mJ/pulse for Bi_2O_3NPs and (500, 600, 700) mJ/Pulse for TeNPs with a positive lens having a focal length of 9 cm. The spot size was about 1.5 mm in diameter and the liquid thickness was changed in the range from 2-14 mm to increase the shock wave and it's adjusted by using different dimension of cells. The number of laser shots applied for the metal target was 20 pulses. Atomic Force Microscope (model AA3000, Angstrom Advance Inc., USA) and Transmission Electron Microscope (CM10-PW6020, Philips, Germany) were used to examine the size and size distributions of the metals NPs[18].

Absorbance spectra of the NPs solution were measured by UV-Vis double beam

spectrophotometer (Cary-100 Conc, Autralia). The NPs concentration were also characterized by Atomic Absorption Spectroscopy (AA-680, shimadzu-Japan).

Serum and saliva samples collection

Blood and saliva samples were obtained from patients with CRF attending the unit of hemodialysis (from Alhyat center for kidney diseases in AL-Karama Hospital, Baghdad, Iraq). Blood samples were left for 20 min. at room temperature; the sera were separated by centrifugation at 1500 xg for 10 min. after collection, then sera were stored at -20ºC until the time of assay. In saliva samples, the CRF patients were asked not to eat or drink for at least an hour. After that they rinsed their mouths several times by water, then waiting for 1-2 min. (for water clearance). Unstimulated saliva were collected in sterilized clear containers. The saliva were centrifuged at 1500 xg for 10 min. and then kept frozen at -20ºC until the time of assay[19,20].

Detection affect's type of Bi_2O_3NPs and TeNPs on T3- binding

ELISA kits for T3-hormone were purchased from human (Wiesbaden, Germany), it is based on the principle of competitive binding between T3 in the test specimen and T3–peroxidase conjugate for a limited number of binding sites on the anti- T3 (sheep) coated well. Thus the amount of T3–peroxidase conjugate bound to the well is inversely proportional to the concentration of T3 in the specimen. After incubation, unbound enzyme conjugate is removed by washing. Tetramethylbenzidin (TMB)/Substrate solution is added, and a blue color develops. The intensity of this color, which changes to yellow after stopping the reaction, is inversely proportional to the amount of T3 in the specimen. The general procedure is summarized as follow with some modification:

Standard solutions containing 0, 0.5, 1.0, 2.5, 5 and 7.5 ng/mL of T3-hormones were used (50 µl for each well) to plotting the standard curve. In other strips 50 µL of serum or saliva (from CRF patients), 10 µL 0f Bi_2O_3NPs or TeNPs was added to calculate the T3 in the presence of NPs; or 10 µL of DDW to calculate the T3 without presence of NPs. Other materials were added as in procedure

The activation and inhibition percentages of binding between antigen and antibody were calculated by comparing the T3 concentration with and without the NPs colloids and under the same conditions, according to the equation:

% Activation = 100 x [T3 in the presence of NPs / T3 in the absence of NPs] - 100

% Inhibition = 100 - 100 x [T3 in the presence of NPs / T3 in the absence of NPs]

Characterization of the T3- binding in the presence of NPs

Determination the optimum concentrations of NPs on T3- binding:

A stock solution (11 ppm) concentration of Bi_2O_3NPs (700 mJ/Pulse) and (10 ppm) concentration of TeNPs (700 mJ/Pulse) and then the following concentrations (9, 7, 5, 3, 1) ppm and (7, 5, 3, 1, 0.5) ppm for each Bi_2O_3NPs and TeNPs, respectively, were prepared by serial dilution from the stock solution with DDW and applied for both serum and saliva samples.

Determination the optimum particle size

A three different particle size of Bi_2O_3NPs (Average diameter: 76.58, 89.04, 75.87 nm) by using different laser energy (500, 600, 700) mJ/Pulse, respectively and TeNPs (Average diameter: 46.53, 44.76, 31.99 nm) by using different laser energy (500, 600, 700) mJ/Pulse, respectively. From the solutions for the three particles size synthesized, Bi_2O_3NPs (2 ppm) and TeNPs (5 ppm) were prepared by diluting with DDW and applied for both serum and saliva samples.

RESULTS AND DISCUSSION

Nanotechnology is a new discipline with many applications in fields like biological sciences and medicine. Nanomaterials are applied as coating materials, as well as in treatment and diagnosis[19]. The PLAL process is currently explored as a prospective top-down (dispersion method) strategy of metals NPs preparation[20]. The preparation of pure noble metals of Bi_2O_3NPs and TeNPs, which addressed in this research, will investigated of the biomedical applications to the commercially available ELISA test.

Characterization of the NPs

An interesting aspect of metal NPs is that their optical properties depend strongly on the particle size and shape. As an example, bulk gold looks yellowish in reflected light, while thin gold films look blue in transmission. This blue color steadily changes to orange as the particle size is decreased to ~ 3 nm. These effects are the result of changes in the Surface Plasmon Resonance (SPR)[21]. Fig. 1 and Fig. 2 show the SPR absorption spectrum of colloidal solutions of Bi_2O_3NPs and TeNPs, respectively. In Fig. 1, the pulse energy at the target surface were varied from (A-500, B-600, C-700) mJ/Pulse for Bi_2O_3NPs, which show the colloidal solution of NPs has absorption lying between 265-275 nm. These Absorption peaks correspond to peak Bi core layer. These results agree with other work[22]. These peaks

have red shift with the increase of laser fluence (increase in particle size). In general a slight increase in the optical absorption as a function of incident light wavelength could be recognized with increasing in laser fluence due to the increase in laser ablation efficiency that means increase in the amount of ablated material (increasing the number of particles inside the colloidal, see Table 1). This result agrees with other work[23]. The UV-Visible spectrum of TeNPs is shown in Fig. 2; a band observed in the spectrum corresponding to SPR, occurred in about 290 nm. The pulses energy at the target surface were varied from (E-500, F-600, G-700) mJ/Pulse, which show increase in the optical absorption as a function of incident light wavelength. The concentrations of both NPs were shown in Table 1 for each pulse energy in liquid, which measured by using atomic absorption spectrophotometer, as a function of standard concentration samples to make the calibration curve.

Table 1: The concentration (ppm) by AAS and the average diameter (nm) by AFM for Bi_2O_3NPs (A, B, C) and TeNPs (D, E, F)

Concentration (ppm)	Average diameter (nm)	Energy (mJ)	Concentration (ppm)	Average diameter (nm)	Energy (mJ)
7.40	46.53	D) Te-500 mJ	2.07	76.58	A) Bi-500 mJ
8.62	44.76	E) Te-600 mJ	9.31	89.04	B) Bi-600 mJ
10.21	31.99	F) Te-700 mJ	11.29	75.87	C) Bi-700 mJ

The results revealed that the concentration of NPs increase with increasing the pulses energy, while the average diameter, in general, decreased, these results in agree with other study[24] for silver NPs generation, which shows that increase of the pulse energy causes a shift of the size distribution maximum from 100 nm to 60 nm. However, it is difficult to explain the generated particles size distribution by only laser fluence because target properties also affect particle size[25]. Fig. 3A and Fig. 3B show the 2D and 3D AFM images and the corresponding size distribution of Bi_2O_3NPs and TeNPs, respectively, by laser ablation of metal immersed in DDW at 20 pulse with different pulse energy. The origin of the surface morphology of the irregularly shaped particles sizes and the size distribution broaden can be explained by absorption with defects and thermally induced pressure pulses which cause cracking[26]. Fig. 4 (A and B) shows the TEM images for Bi_2O_3NPs (700 mJ/Pulse) and TeNPs (700 mJ/Pulse), respectively. The NPs thus produced were calculated to have the average diameters range of 70-75 nm (in agree with AFM) and 40-50 nm, respectively.

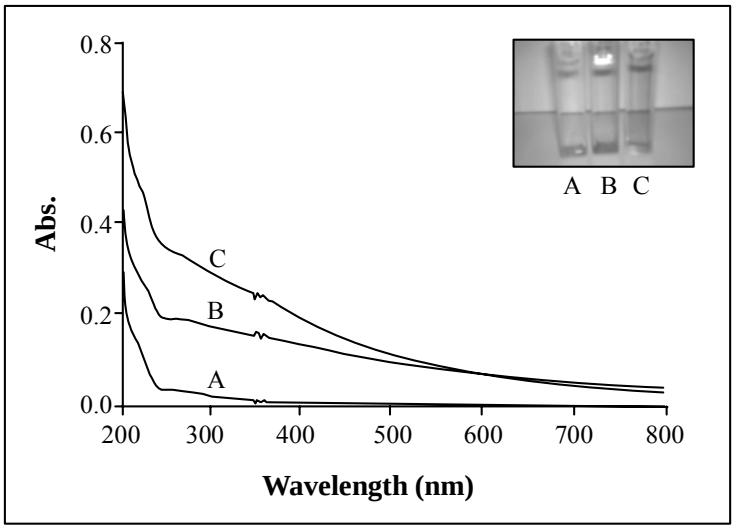

Fig. 1: UV-Vis spectrum and optical picture of Bi_2O_3NPs obtained immediately after laser ablation of metal plates immersed in DDW with laser energy of (A-500 mJ/Pulse, B-600 mJ/Pulse, C-700 mJ/Pulse) laser shots of 20 pulses and wave length is 1064 nm of Nd : YAG

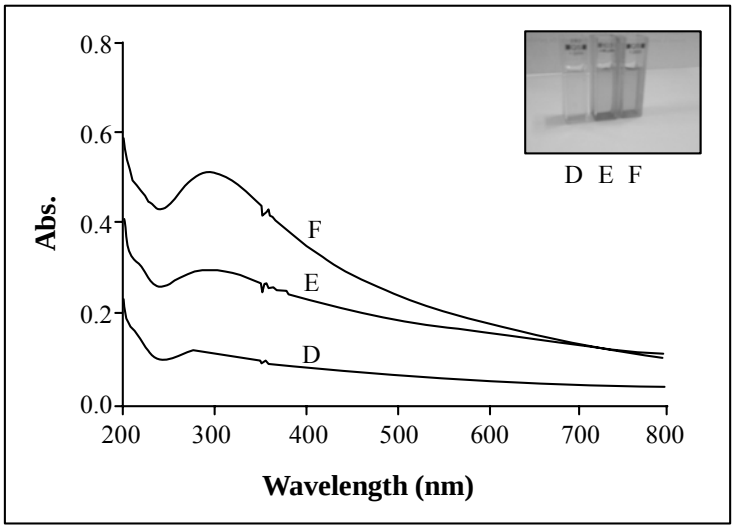

Fig. 2: UV-Vis spectrum and optical picture of TeNPs obtained immediately after laser ablation of metal plates immersed in DDW with laser energy of (D-500 mJ/Pulse, E-600 mJ/Pulse, F-700 mJ/Pulse) laser shots of 20 pulses and wave length is 1064 nm of Nd : YAG

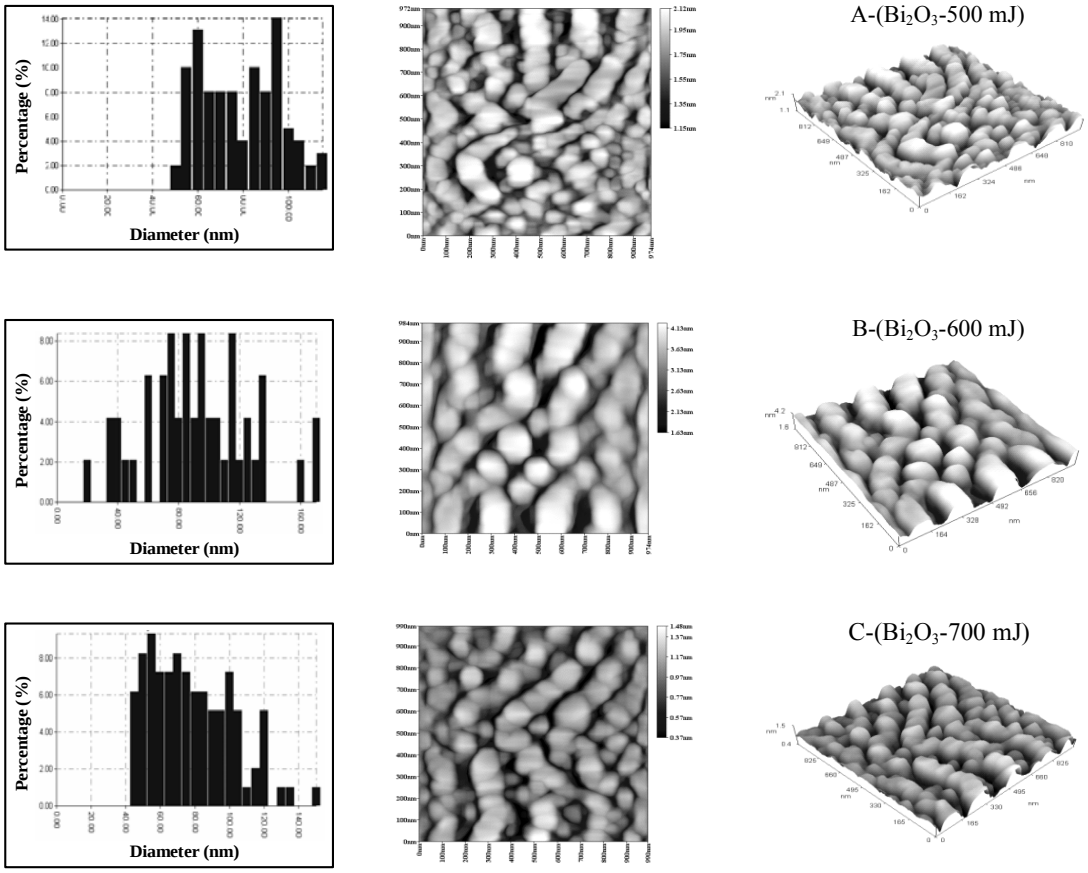

Fig. 3A: AFM images and size distributions of Bi_2O_3NPs, obtained by laser ablation of metal plats immersed in DDW with laser energy of (A-500 mJ/Pulse, B-600 mJ/Pulse, C-700 mJ/Pulse) laser shots of 20 pulses and wave length is 1064 nm of Nd : YAG

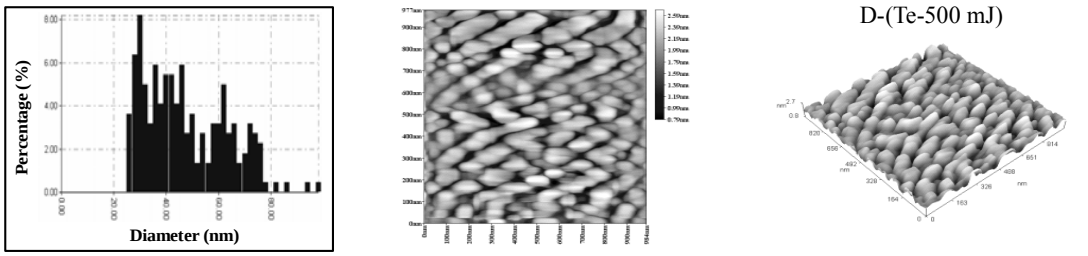

Cont…

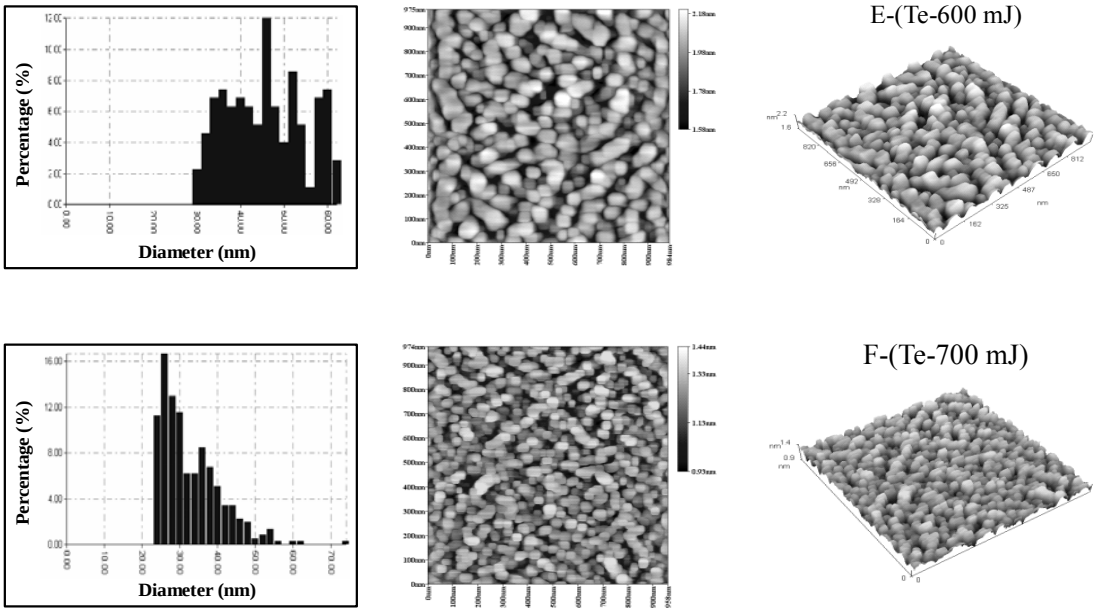

Fig. 3B: AFM images and size distributions of TeNPs, obtained by laser ablation of metal plats immersed in DDW with laser energy of (D-500 mJ/Pulse, E-600 mJ/Pulse, F-700 mJ/Pulse) laser shots of 20 pulses and wave length is 1064 nm of Nd : YAG

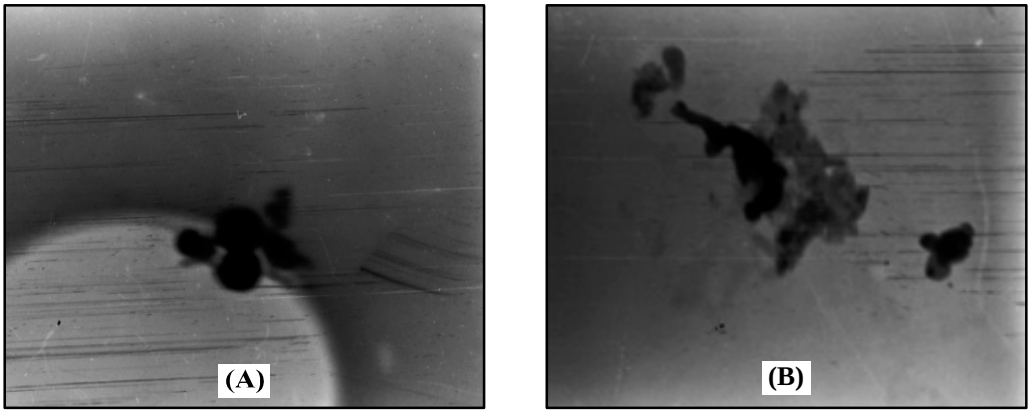

Fig. 4: TEM images of (A) Bi_2O_3NPs (700 mJ/Pulse) and (B) TeNPs (700 mJ/Pulse), obtained by laser ablation of metal plats immersed in DDW with laser shots of 20 pulses and wave length is 1064 nm of Nd : YAG

Optimization of the assay condition

The interaction between proteins and some NPs depends upon three separate but dependent phenomena: a) Ionic attraction between the negatively charged gold and the positively charged proteins; b) Hydrophobic attraction between the Antibody and the gold surface; c) Dative binding between the gold conducting electrons and sulfur atoms which may occur with amino acids of the proteins[16]. The conjugation process is, therefore, influenced greatly by different conditions. The effects of presence NPs on the levels of T3 in serum and saliva patients with CRF whose their thyroid had disorder (hypothyroidism) showed different effect (Activation or Inhibition) by using the same kit conditions mentioned in experimental work with adding 10 µL of NPs.

In studying the effect of different concentrations of Bi_2O_3NPs (700 mJ/Pulse) on serum and saliva samples, which shown in Fig. 5 (A and B), respectively. It can be seen that, the highest assay of Activation to binding T3 was in serum achieved when the Bi_2O_3NPs concentration at 7 ppm, with 57.75 percentage of Activation as compare to saliva samples, which was 7 ppm with 12.05 percentage of Inhibition. In TeNPs Fig. 6 (A and B), it can be seen that, less than 1 ppm with 24.06 percentage of Inhibition, while it is 1 ppm with 47.92 percentage of Inhibition for serum and saliva samples, respectively.

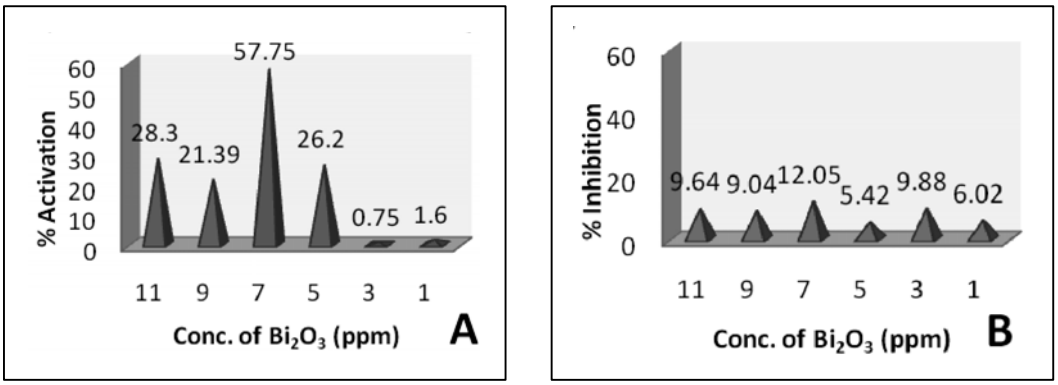

Fig. 5: Optimization of the concentration of (A) Bi_2O_3NPs (700 mJ/Pulse) on serum specimen and (B) Bi_2O_3NPs (700 mJ/Pulse) on saliva specimen, to be used in the ELISA test. Other condition: 50 µL serum or saliva specimen; 10 µL of NPs (1-11 ppm) or DDW; 100 µL working conjugate solution; incubation time 1hr at 20-25ºC; 100 µL substrate reagent solution; incubaton time 15 min. at 20-25ºC; 50 µL stop solution

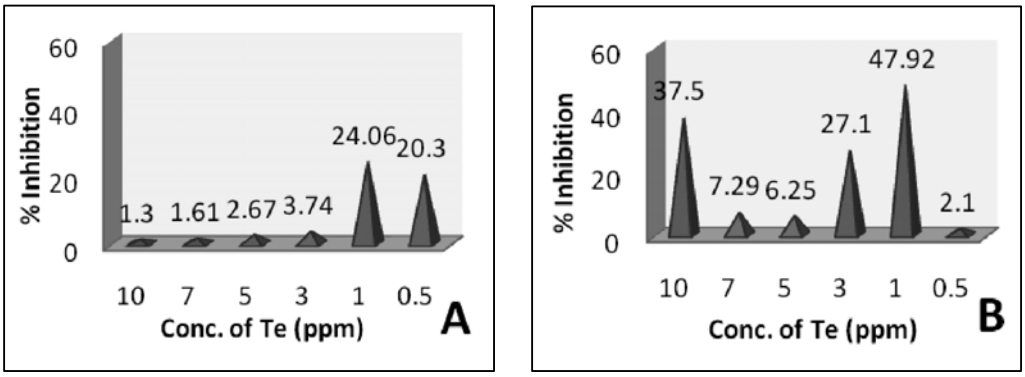

Fig. 6: Optimization of the concentration of (A) TeNPs (700 mJ/Pulse) on serum specimen and (B) TeNPs (700 mJ/Pulse) on saliva specimen, to be used in the ELISA test. Other condition: 50 µL serum or saliva specimen; 10 µL of NPs (1-10 ppm) or DDW; 100 µL working conjugate solution; incubation time 1 hr at 20-25ºC; 100 µL substrate reagent solution; incubation time 15 min. at 20-25ºC; 50 µL stop solution

The effect of different particle size of Bi_2O_3NPs was shown in Fig. 7 (A and B), for both serum and saliva samples, respectively. As can be seen, the 75.87 nm (smallest particle size) was the highest effective for Activation and Inhibition with 17.65 and 12.1 for serum and saliva samples, respectively.

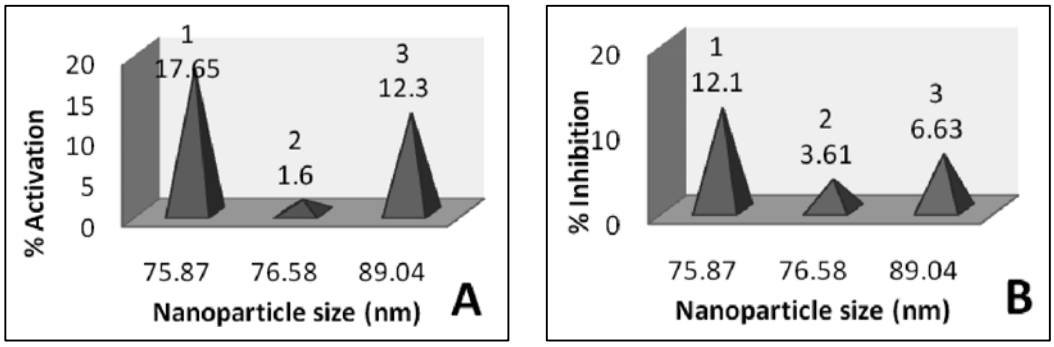

Fig. 7: The effect of different particle size on the binding T3 of (A) Bi_2O_3NPs (1-700 mJ/Pulse; 2-500 mJ/Pulse; 3-600 mJ/Pulse) on serum specimen and (B) Bi_2O_3NPs (1-700 mJ/Pulse; 2-500 mJ/Pulse; 3-600 mJ/Pulse) on saliva specimen, to be used in the ELISA test. Other condition: 50 µL serum or saliva specimen; 10 µL of NPs (2 ppm for all Bi_2O_3NPs) or DDW; 100 µL working conjugate solution; incubation time 1hr at 20-25ºC; 100 µL substrate reagent solution; incubation time 15 min. at 20-25ºC; 50 µL stop solution

Also TeNPs in Fig. 8 (A and B), shown 31.99 nm (smallest particle size) was the highest effective with percentage of Inhibition 5.3 and 7.35 for serum and saliva samples, respectively. Therefore, as the particle size decreases the binding of hormone to its receptor increased (in Activation) or decreased (in Inhibition), which agrees with other study[27] showed that smaller particles would greatly speed up the binding when it's used the polystyrene NPs with europium chelate as fluorescent reporters in an immunoassay for atrazine.

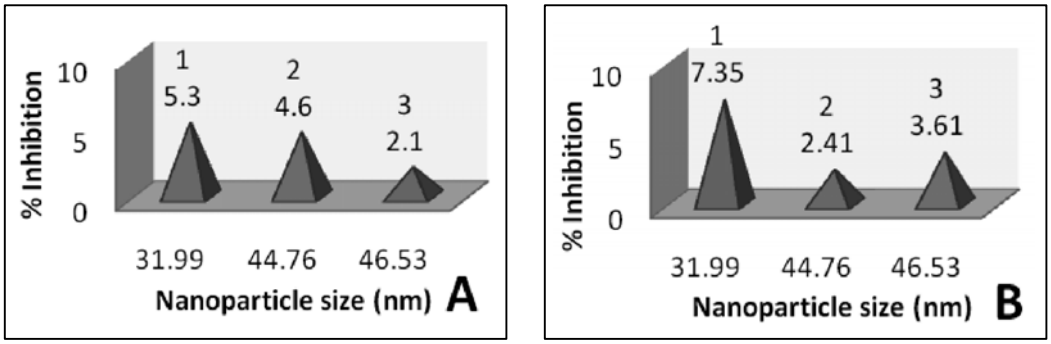

Fig. 8: The effect of different particle size on the binding T3 of (A) TeNPs (1-700 mJ/Pulse; 2-600 mJ/Pulse; 3-500 mJ/Pulse) on serum specimen and (B) TeNPs (1-700 mJ/Pulse; 2-600 mJ/Pulse; 3-500 mJ/Pulse) on saliva specimen, to be used in the ELISA test. Other condition: 50 µL serum or saliva specimen; 10 µL of NPs (5 ppm for all TeNPs) or DDW; 100 µL working conjugate solution; incubation time 1 hr at 20-25ºC; 100 µL substrate reagent solution; incubation time 15 min. at 20-25ºC; 50 µL stop solution

The advantages of NPs are their high surface-to-volume ratios, their quantum confinement, and their nanoscale size, which allow more active site to interact with biological systems[4]. This phenomenon needs to be further studied to determine the optimal particle size for binding the Antibody/Antigen and subsequently for other molecules of interest.

CONCLUSION

In this work, we have presented easy method for the preparation of Bi_2O_3NPs and TeNPs with well-defined size and shape. Optical measurements of colloidal NPs exhibit maximum optical extinction lying between 265-275 nm and at around 290 nm for Bi_2O_3NPs and TeNPs, respectively. The results revealed that the concentration of NPs increase with an increase in pulses energy, while the average diameter (nm), in general, will decrease. Average size, size distribution, and morphology of NPs were studied by using AFM, TEM.

Bi_2O_3NPs showed an activation effect on the binding between anti-T3 antibody and antigen-T3 in the serum samples, while, it was Inhibition effect, when saliva used. Also, the TeNPs showed the Inhibition effect, when both samples were used. We hypothesized that NPs of Bi and Te interact with functional groups of Anti-T3 antibody, resulting in protein denaturation and so NPs of Bi and Te activated or inhibited the binding between antibody and antigen. Specifically, we were able to demonstrate that as the particle size decreases the effect for binding of the assay is increased. To the best of our knowledge, the present work is the first study that demonstrate the effect of Bi_2O_3NPs and TeNPs colloids on this binding, therefore, a more accurate analytical procedure should be developed in order to avoid misjudgments, in order to used of these NPs in biomedical applications such as the treatment and follow up by adjustment the levels of T3-hormones of patients suffered from thyroid disorder.

ACKNOWLEDGEMENT

The authors thank (Al-Mustansyria University, College of Science, Chemistry Dept.) for AAS measurements; (Al-Nahrain University) for their helpful in TEM measurements; (ALHYAT center for kidney diseases in AL-KARAMA Hospital) for collection of samples; Dr. K. A. Abdulrahman (University of Technology, Dept. of Applied Science) for assistant in nanoparticles preparations.

REFERENCES

1. V. D. Timothy, Applications of Nanotechnology in Food Packaging and Food Safety: Barrier Materials, Antimicrobials and Sensors, J. Colloid and Interface Sci., **363**, 1-24 (2011).
2. F. Stanley Rosarin and S. Mirunalini, Nobel Metallic Nanoparticles with Novel Biomedical Properties, J. Bioanal. Biomed., **3(4)**, 85-91 (2011).
3. M. S. Singh, Manikandan and A. K. Kumaraguru, Nanoparticles: A New Technology with Wide Applications, Res. J. Nanosci. Nanotechnol., **10**, 1996-2014 (2010).
4. H. Rene, V. Donaji, D. David, A. Katiushka, G. Marianela, A. D. G. Myriam and C. Claudio, Zerovalent Bismuth Nanoparticles Inhibit *Streptococcus Mutans* Growth and Formation of Biofilm, Int. J. Nanomedicine, **7**, 2109-2113 (2012).
5. M. Dechong, Z. Jingzhe, C. Rui, Y. Shanshan, Z. Yan, H. Xinili, L. Linzhi, Z. Li, L. Yan and Y. Chengzhong, Novel Synthesis and Characterization of Bismuth Nano/microcrystals with Sodium Hypophosphite as Reductant, Advanced Powder Technology, **24**, 79-85 (2013).

6. Z. Bijan, A. F. Mohammad, S. Zargham, S. Mojtaba, R. Sassan and R. S. Ahmad, Biosynthesis and Recovery of Rod-shaped Tellurium Nanoparticles and their Bactericidal Activities, Materials Research Bulletin, **47**, 3719-3725 (2012).

7. A. B. Lalla, D. Mandy, J. Vincent and J. Claus, Tellurium: An Element with Great Biological Potency and Potential, Org. Biomol. Chem., **8**, 4203-4216 (2010).

8. K. A. Abdulrahman and N. R. Dayah, Preparation of Silver Nanoparticles by Pulsed Laser Ablation in Liquid Medium, Eng. & Tech. J., **29 (15)**, 3058-3066 (2011).

9. P. Liu, Y. Liang, H. B. Li and G. W. Yang, Laser Ablation in Liquid: from Nanocrystals Synthesis to Nanostructures Fabrication, J. Nanomaterials Applications and Properties, **1**, 133-141 (2011).

10. V. S. Lim, Thyroid Function in Patients with Chronic Renal Failure, Am. J. Kidney Dis., **38** [Suppl. 1], S80-S84 (2001).

11. M. Jolanta, M. Jacek, W. Slawomir and M. Michal, Adiponectin, Leptin and Thyroid Hormones in Patients with Chronic Renal Failure and on Renal Replacement Therapy: are they Related, Nephrol. Dial.Transplant, **21**, 145-152 (2006).

12. A. S. Pon, B. Zachariah, N. Selvaraj and R. Vinayagamoorthi, An Evaluation of Thyroid Hormone Status and Oxidative Stress in Undialyzed Chronic Renal Failure Patients, Indian J. Physiol. Pharmacol., **50 (3)**, 279-284 (2006).

13. A. Marcelo, N. Tetsuji and E. James, The Salivary Gland Fluid Secretion Mechanism, The J. Med. Investigation, **56**, 192-196 (2009).

14. H. A. Raghad, Evalution of Sex Steroid Hormones & Inflammatory Biomarker in Plaque Associated Gingivitis, MSc thesis, University of AL-Mustansiriyah, College of Science (2012) pp. 2-7.

15. R. M. Nagler, Saliva Analysis for Monitoring Dialysis and Renal Function, Clin. Chem., **54 (9)**, 1415-1417 (2008).

16. A. Ambrosi, F. Airo and A. Merkoci, Enhanced Gold Nanoparticle Based ELISA for a Breast Cancer Biomarker, Anal. Chem., **82**, 1151-1156 (2010).

17. I. M. Kennedy, M. Koivunen, S. Gee, C. Cummins, R. Perron, D. Dosev and B. D. Hammock, Nanoscale Fluoro-immuno Assays with Lanthanide Oxide Nanoparticles, Proc. of SPIE, **5593**, 329-339 (2004).

18. H. Frank, B. S. David and T. Frank, Determination of Morphological Parameters of Supported Gold Nanoparticles: Comparison of AFM Combined with Optical Spectroscopy and Theoretical Modeling Versus TEM, Appl. Sci., **2**, 566-583 (2012).

19. V. L. Colvin, The Potential Environmental Impact of Engineered Nanomaterials, Nat. Biotechnol., **21(10)**, 1166-1170 (2003).

20. A. Pyatenko, M. Yamaguchi and M. Suzuki, Laser Photolysis of Silver Colloid Prepared by Citric Acid Reaction Method, J. Phys. Chem., **109**, 21608-21611 (2005).

21. U. Kreibig and M. Vollmer, Optical Properties of Metal Clusters, **Vol. 25**, Springer Series in Materials Science, Springer-Verlag, Berlin, Germany, Ch. 4 (1995) p. 312.

22. J. Li, H. Q. Fan, J. Chen and L. Liu, Synthesis and Characterization of Polyvinyl Pyrrolidone-capped Bismuth Nanospheres, J. Physicochem. Eng. Aspects, **340**, 66-69 (2009).

23. A. V. Kabashina and M. Meunier, Synthesis of Colloidal Nanoparticles During Femtosecond Laser Ablation of Gold in Water, J. Appl. Phys., **94**, 7941-7946 (2003).

24. H. Anne, B. Stephan and N. Chichkov, Influences on Nanoparticle Production During Pulsed Laser Ablation, JLMN-J. Laser Micro/Nanoeng., **3 (2)**, 73-77 (2008).

25. T. Nishi, A. Takeichi, H. Azuma, N. Suzuki, T. Hioki and T. Motohiro, Fabrication of Palladium Nanoparticles by Laser Ablation in Liquid, JLMN-J. Laser Micro/ Nanoeng., **5 (3)**, 192-196 (2010).

26. O. R. Musaev, A. E. Midgley, J. M. Wrobel and M. B. Kruger, Laser Ablation of Alumina in Water, Chemical Physics Letters, **487**, 81-83 (2010).

27. C. Jin, T. Jinhai, Y. Feng and L. Huangxian, A Gold Nanoparticles/Sol-gel Composite Architecture for Encapsulation of Immunoconjugate or Reagentless Electrochemical Immunoassay, Biomaterials, **27**, 2313-2321 (2006).

Accepted : 19.07.2013